ADVANCED FUNCTIONAL MATERIALS
www.afm-journal.de

Intrinsically Thermally Degradable Microstructures Fabricated by Photodimerization in Rapid 3D Laser Printing

Steven C. Gauci, Paul Somers, Mohammed Aljuaid, Martin Wegener, Christopher Barner-Kowollik, and Hannes A. Houck**

Classical photoresists utilized in direct laser writing (DLW) rely on photoinitiators and radical polymerization mechanisms to induce the cross-linking process. Herein, a simple initiator-free photoresist is introduced that enables the rapid fabrication of intrinsically thermally degradable 3D microstructures via DLW. The reported photoresist exploits the [2 + 2] photo-dimerization reaction of a multifunctional monosubstituted thiomaleimide compound while harvesting on-demand microstructure degradation through the intrinsic thermally reversible nature of the photocrosslinks. The photoresist exceeds attainable DLW printing speeds for non-chain growth resins, readily attaining 1500 µm s^{-1} and up to 5000 µm s^{-1}, making it a promising system to compete with traditional photo-initiator containing resists while introducing on-demand post-printing degradability.

1. Introduction

Direct laser writing (DLW) has become one of the most versatile, and routinely used additive manufacturing techniques for the fabrication of 3D structures on the microscopic scale.[1–4] DLW exploits two-photon absorption (TPA), whereby a femtosecond pulsed laser is tightly focused into the volume of a photoresist. Consequently, the laser writing process is constrained to a very small volume element – called a voxel – and accumulation effects in the periphery are suppressed thus enabling the fabrication of near-arbitrary 3D structures with sub-100 nm scale features.[5] As a result, DLW has been employed to fabricate highly resolved structures that have been utilized for applications ranging from microfluidics,[6] to photonics,[7] to cell biology.[8,9]

Classically, DLW is an additive approach and thus often restricted to the fabrication of permanent structures, which arise from the use of photoresists that are irreversibly cross-linked.[10] For many applications, however, the ability to erase the 3D structure – or parts of it – once the printing is complete is an important requirement.[11] For example, post-DLW erasing can be used for the removal of support materials after printing overhanging features,[12] for the degradation of cellular scaffolds to trigger cell release,[13] and for the cleavage of valves and bridges in fluidic devices.[14] To achieve these aims, establishing advanced photoresists that can be cleaved on-demand with simple orthogonal procedures is essential.

Traditional photoresists employed in DLW often rely on photoinitiator species to trigger chain-growth reactions that convert a liquid formulation of low molecular weight compounds (e.g., monomers, oligomers, cross-linkers) into a covalently linked solid network material.[15,16] While photoinitiators play a key role in the printing process, careful consideration is needed due to their possible toxicity and sensitivity to oxygen.[17,18] In contrast, initiator-free photoresists typically cannot benefit from rapid chain propagation mechanisms to initiate network formation during the printing process. Thus, photoresists cured via non-chain growth polymerizations, i.e., based on photocycloadditions, typically display reduced photosensitivity and examples of initiator-free 3D printing systems are rare.[19–21] This fundamental challenge translates into much slower writing speeds in comparison to other initiator-free resists, such as those based on C,H- insertion cross-linking,[22] as well as their

S. C. Gauci, C. Barner-Kowollik
School of Chemistry and Physics, Centre for Materials Science
Queensland University of Technology (QUT)
2 George Street, Brisbane, QLD 4000, Australia
E-mail: christopher.barnerkowollik@qut.edu.au

S. C. Gauci, P. Somers, M. Wegener, C. Barner-Kowollik
Institute of Nanotechnology (INT)
Karlsruhe Institute of Technology (KIT)
Kaiserstraße 12, 76131 Karlsruhe, Germany

M. Aljuaid
Department of Chemistry
Turabah University College
Taif University
P.O. Box 11099, Taif 21944, Saudi Arabia

M. Wegener
Institute of Applied Physics (APH)
Karlsruhe Institute of Technology (KIT)
Kaiserstraße 12, 76131 Karlsruhe, Germany

H. A. Houck
Photochemistry for Materials Group
Department of Chemistry
University of Warwick
Library Road, Coventry CV4 7AL, UK
E-mail: hannes.houck@warwick.ac.uk

The ORCID identification number(s) for the author(s) of this article can be found under https://doi.org/10.1002/adfm.202414713

DOI: 10.1002/adfm.202414713

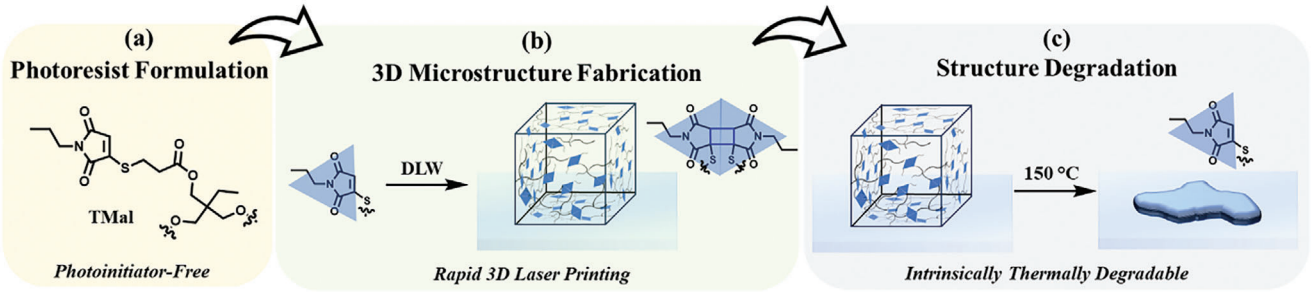

Figure 1. Overview of the present study. a) A 3-arm monothiomaleimide utilized as a dissolve-and-go initiator-free photoresist for b) 3D direct laser writing of microstructures through a [2 + 2] photodimerization, resulting in c) intrinsically, thermally degradable prints.

initiator-containing counterparts, both of which are capable of printing at writing speeds (far) exceeding 1000 µm s^{-1}. For example, Werner et al. reported microstructure fabrication via the [2 + 2] cycloaddition of multi-maleimide monomers under TPA conditions, employing a writing speed of 15 µm s^{-1}.[23] Meanwhile, the photoinduced [4 + 2] cycloaddition between triazolinedione and naphthalene was exploited to fabricate microstructures via TPA, which required even slower writing speeds of 10 µm s^{-1}, likely attributed to the transient reversible nature of the cycloadducts at ambient printing temperatures.[24,25] Most recently, printing speeds well above 1000 µm s^{-1} have been obtained making use of a chalcone-based [2 + 2] photodimerization, albeit in the presence of a photosensitizer, at low concentrations and with varying printing quality.[26] These examples highlight several advantages of the exclusion of a radical photoinitiator, amongst them the ability to design microstructures with a highly pre-defined network topology.[27] Another key potential advantage of utilizing non-chain growth mechanisms such as photocycloadditions for 3D printing applications is that the resulting photoaddition products may be reversible.[28–31] Thus, the use of cycloadditions in DLW provides an attractive avenue toward fabricating microstructures that can be erased post-printing and on-demand through the corresponding cycloreversion process.

Herein, we present a photoinitiator-free photoresist for DLW based on a photocycloaddition mechanism that allows for an up to 100-fold faster fabrication of 3D microstructures compared to state-of-the-art cycloaddition inks, attaining writing speeds similar to conventional DLW resists based on chain-growth processes. Additionally, the fabricated structures can be intrinsically erased post-printing without the need for chemical treatment or external stimuli other than elevated temperature (**Figure 1**). Specifically, we introduce a new photoresist based on the recently emerged monothiomaleimide photodimerization chemistry,[32] whereby the ink consists of only a 3-arm monothiomaleimide monomer in solution (**TMal**, Figure 1a). Unlike conventional maleimides, thiomaleimide derivatives have recently been shown to display more efficient photoreactivity with the swift formation of [2 + 2] photodimer products,[33] which is demonstrated herein to result in vastly improved two-photon laser printing speeds. Moreover, the resulting photodimers have recently been reported to thermally revert back to the initial monomers when heated above 120 °C both in solution and under bulk conditions,[34] which is exploited to degrade the printed structures when heated at 150 °C (Figure 1b-c).

2. Results and Discussion

2.1. Printing Performance

Inspired by the conventional maleimide system employed by Werner et al.,[23] we posed the question of whether thiomaleimides would also undergo TPA and therefore be applicable to additive manufacturing based on DLW.[35] Thus, a photoresist was prepared by dissolving a 3-arm monothiomaleimide in propylene carbonate (**TMal**, c = 750 mg mL^{-1}, refer to Sections S3 and S4 (Supporting Information) for synthetic and experimental details). Propylene carbonate was selected as a suitable printing matrix to lower the viscosity of the monomer while preventing solvent evaporation during printing. To explore the range of printing parameters achievable with the **TMal** photoresist, an array of simple cone-shaped microstructures was fabricated with laser powers varying from 15 and 35 mW and scan speeds ranging from 500 to 1500 µm s^{-1}, respectively (Figure S2a, Supporting Information). Remarkably, the current photoresist exhibits a >100 fold-increase in printing speed compared to the previously mentioned multi-maleimide and triazolinedione/naphthalene photoresists utilized in DLW. Intrigued by these vastly improved printing speeds, further investigations into the maximum speed the **TMal** resist can achieve revealed that printing remains possible even at a scan speed of 5000 µm s^{-1} (Figure S2b, Supporting Information).

Having established the printability of the **TMal** resist using a two-photon laser printer, the optimal printing parameters were then determined. For this, an array of distinctive blocks with overall dimensions of 20 µm × 20 µm × 5 µm was printed from the **TMal** photoresist with laser powers and scan speeds between 15 and 35 mW and 500 and 1500 µm s^{-1}, respectively (**Figure 2a**, also refer to Figure S3, Supporting Information). Within this range, an optimal variability of printing parameters was observed, producing sufficient cross-linking at a low exposure dose yet did not cause micro-explosions at a higher exposure dose. By making a judicious selection of the block design, the printing results could be assessed via scanning electron microscopy (SEM) imaging (Figure 2a), from which a relevant laser power and scan speed could be identified. As depicted in Figure 2a, the optimal printing parameters for the photoresist were obtained at a laser power of 20 mW (laser intensity of 8.2 TW cm^{-2}), and at a scan speed of 1250 µm s^{-1} for the block structures. To investigate the obtainable feature size and lateral resolution of the photoresist at these selected printing parameters (i.e., 20 mW and 1250 µm s^{-1}), lines

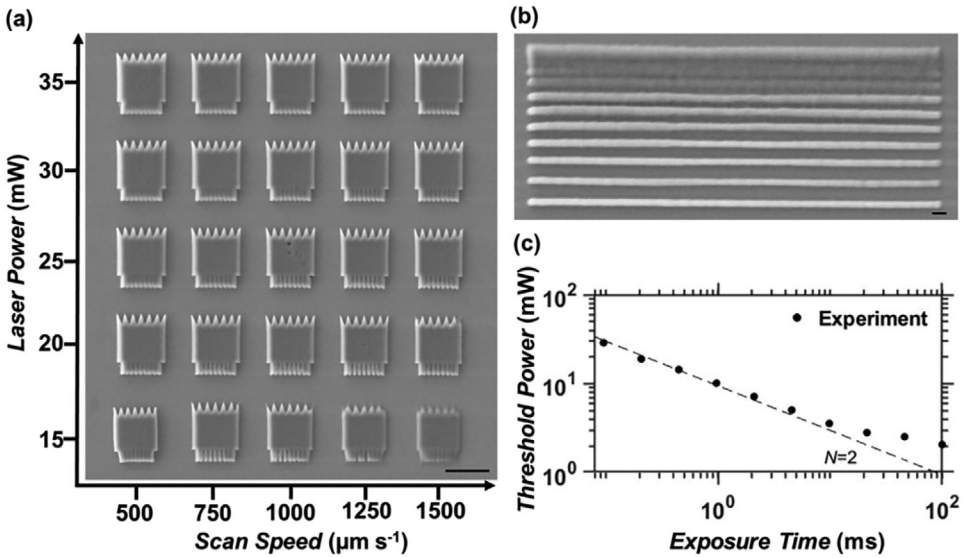

Figure 2. SEM images of microstructures fabricated via DLW from the **TMal** photoresist. a) Distinctive block array printed with laser powers between 15 and 35 mW (y-axis), and scan speeds between 500 and 1500 μm s^{-1} (x-axis). Scale bar = 20 μm. b) Lines demonstrating a feature size and lateral resolution of 300 nm. Scale bar = 1 μm. c) Double-logarithmic plot of threshold printing power during point exposure for increasing exposure times. Dashed line is a guide to the eye for a nonlinear response of $N = 2$.

with different spacing were printed. A feature size of 300 nm and line separations as close as 300 nm were achieved (Figure 2b). We note, however, that smaller features sizes can be achieved under tailored conditions. For example, isolated linewidths of ≈160 nm could be achieved at a printing speed of 100 μm s^{-1} and a laser power of 4.75 mW (laser intensity of 0.124 TW cm^{-2}, also see Figure S4, Supporting Information). This feature size is comparable with conventional two-photon resists, such as Nanoscribe's IP Photoresins, while still an order of magnitude faster than previous cycloaddition-based inks.

Finally, as it is possible that there could be higher order nonlinear processes contributing to the mechanism of printing, we evaluate the degree of nonlinear absorption of the **TMal** resist using a point exposure test. It is known that the nonlinear response of a resist can be investigated by probing the threshold laser power for polymerization as a function of exposure time.[36] Specifically, that relationship is given by $P_{Th} \propto (\Delta t)^{-1/N}$, where P_{Th} is the threshold laser power for printing, Δt is the exposure time of the resist, and the integer N is the order of the nonlinearity. We determined the threshold power for printing using pointwise exposures (i.e., stationary laser focus) for exposure times spanning several orders of magnitude. The results are plotted in Figure 2c on a double-logarithmic plot. For comparison, we include a dashed line indicating an $N = 2$ nonlinear process, expected for a two-photon absorption printing process. The experimental data agrees well with the slope of the dashed line, indicating that the **TMal** resist polymerizes primarily under two-photon absorption in these conditions. Interestingly, at short enough exposure times, no polymerization was observed for the powers tested (up to 50 mW). The smallest exposure time that exhibited some photo-polymerization was 44 μs, however, point exposure printing was unsuccessful to give clean prints and proceeded with an undefinable threshold. A comparison of the 44 μs exposure test and a more typical result of the point exposure test (at 95 μs) is shown in Figure S5 (Supporting Information). The observed poor printing performance at very short exposures of 44 μs is rather surprising, but could be caused by solvent vaporization resulting from the high pulse intensities. Toward longer exposures times, i.e., >10 ms, the resist starts to exhibit a higher-order nonlinear response, a behavior previously observed for free radical-based photoresists and attributed to oxygen diffusion.[36] While the thiomaleimide photodimerization has been observed to be rather inert to oxygen interference, the **TMal** resist may be similarly affected by oxygen diffusion during femtosecond laser irradiation conditions.

2.2. Thermal Degradation and Material Properties

Given the recently reported thermal reversibility of the [2 + 2] cycloaddition of thiomaleimides and their use to create intrinsically recyclable thermoset materials,[34] we first examined whether the structures fabricated via DLW were similarly prone to thermal reversion that would result in the de-cross-linking of the printed material. Therefore, cone-shaped microstructures were fabricated with varying laser powers and scan speeds (i.e., 15 to 35 mW and 500 to 1500 μm s^{-1}, respectively), and subsequently placed in an oven pre-heated to 150 °C for 24 hrs. Through SEM analysis conducted on the cone structures post-printing and following their exposure to 150 °C for 24 hrs, we were able to qualitatively confirm that the structures de-cross-linked and are thus thermally degradable (refer to Figure S6, Supporting Information). The selected degradation temperature of 150 °C was chosen to exclude degradation of the **TMal** organic substrate while still resulting in appropriate bulk degradation kinetics.[34]

Having established that the structures are indeed thermally degradable, we proceeded to measure the mechanical properties of the direct-laser-written material post-printing and during

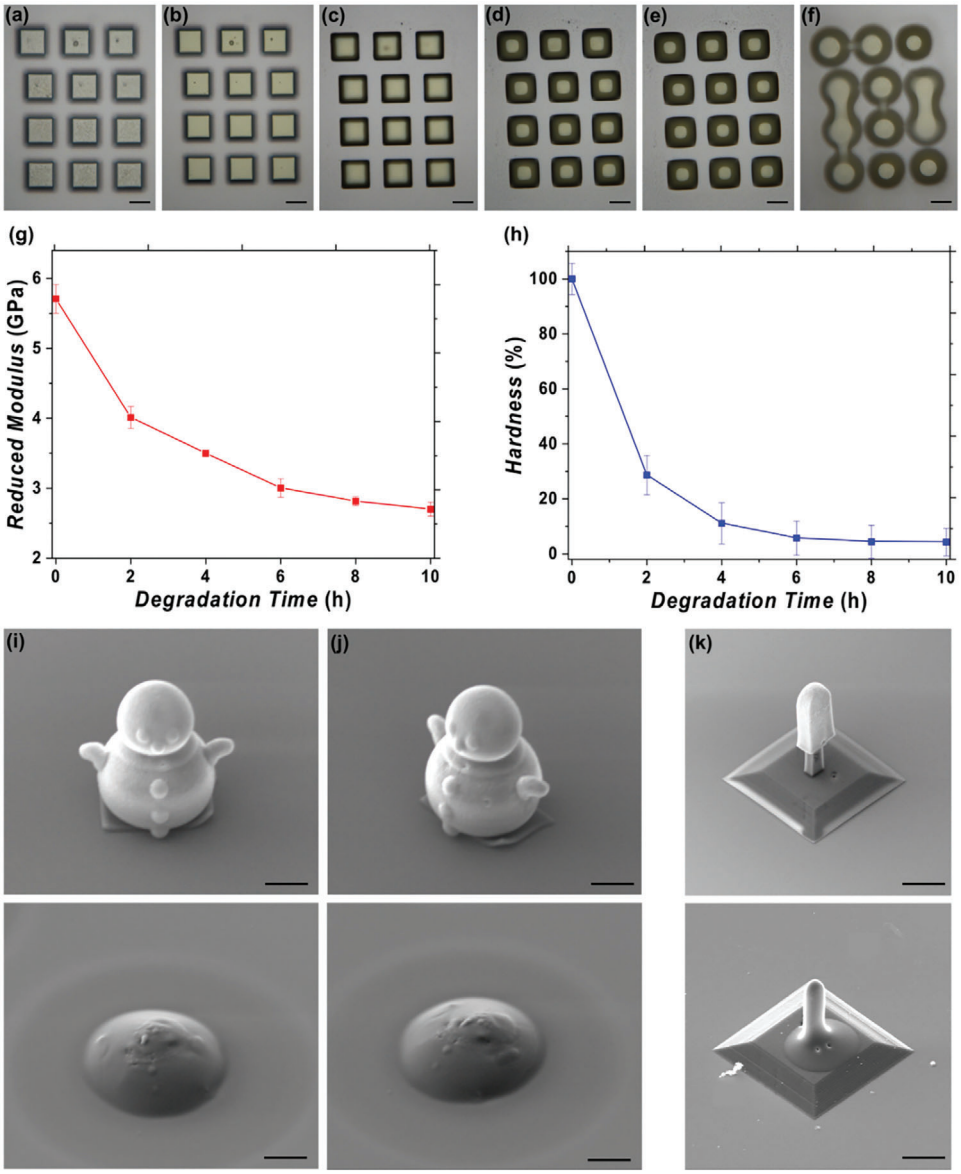

Figure 3. a–f) Optical microscopy images of blocks printed with a laser power of 20 mW and scan speed of 1250 µm s^{-1} post-printing (a) and at 2 h intervals following heating at 150 °C (b–f). g,h) Mechanical properties (reduced modulus and hardness, respectively) determined using nanoindentation of the printed blocks over the course of heating at 150 °C for 10 h. Each data point represents the average of three measurements and the error bars indicate the standard deviation of the data. i,j) SEM images of a snowman printed exclusively from the **TMal** photoresist from different perspectives (top) and after being exposed to 150 °C for 24 h (bottom). k) SEM images of a multi-material structure consisting of segments printed from a non-degradable resist (IPS-Nanoscribe, which forms the base and popsicle-stick segments), as well as the **TMal** photoresist (popsicle segment) post-printing (top) and after 24 h at 150 °C, whereby only the popsicle segment degrades (bottom). Scale bars = 20 µm.

degradation. Therefore, square blocks with dimensions of 30 µm × 30 µm × 10 µm were printed and analyzed via nanoindentation. **Figure** 3a–f depicts the change in shape the blocks underwent in response to placing the microstructures in an oven at a temperature of 150 °C over the course of 10 h. Notably, the blocks exhibit melting and/or flowing behavior during the decross-linking process, which causes them to lose their original square-shape and take on a more rounded form. Their shape alteration coincides with the evolution of the materials' mechanical properties. Initially, the printed blocks exhibited a reduced modulus of 5.71 GPa (Figure 3g), which rapidly decreased to 4.01 GPa after being exposed for 2 hrs at 150 °C. Over the subsequent 8 h timeframe, the reduction in modulus proceeds at a notably slower rate, resulting in a final reduced modulus of 2.71 GPa obtained after 10 h. It should be noted that while the structures degrade, a significant reduction in the remaining material height adds uncertainty over the reduced moduli values with substrate effects becoming no longer negligible. Nonetheless, the clear decay in modulus during the nanoindentation along with the optical microscopy monitoring supports the intrinsic thermal degradation of the laser-written structures. The average hardness of the blocks exhibits a similar trend to the reduced modulus, whereby

a rapid decrease of up to 70% is observed within the first 2 h, followed by a significantly slower decline of only 15% over the next 8 h period (Figure 3h, also refer to Sections S2.4 and Section S5, Supporting Information).

Although mono-thiomaleimide cross-linkers undergo [2 + 2] photo-dimerization under single-photon absorption,[34,35] the same irradiation conditions may not directly translate to a two-photon printing process. Therefore, additional molecular characterization of the actual direct-laser-written structures was performed to verify that laser printing occurred through the previously established photo-induced [2 + 2] cycloaddition reaction. Specifically, square blocks (40 µm × 40 µm × 10 µm) were printed from the **TMal**-based resist and analyzed by infrared spectroscopy. The results confirmed that both [2 + 2] photo-dimerization and the corresponding thermal cycloreversion reactions take place in the structures fabricated via TPA, as evidenced by the almost quantitative reduction and subsequent reappearance of the thiol-substituted C=C stretch at 1556 cm^{-1} after printing and heating, respectively (Figure S8, Supporting Information).

2.3. Proof-Of-Principle of Thermally Degradable 3D Microstructures

To demonstrate the photoresist's ability to fabricate 3D thermally degradable structures, two demonstrator experiments were conducted. In the first example, a micro-sized snowman was fabricated exclusively from the **TMal** photoresist with a laser intensity and scan speed of 20 mW and 1250 µm s^{-1}, respectively (Figure 3i,j). SEM imaging of the snow-man post-printing revealed the resist's ability to fabricate a fully 3D structure (Figure 3i,j, top). Furthermore, when exposed to 150 °C for 24 h, the snowman undergoes a fascinating transformation, taking on a "melted" appearance after de-cross-linking, as illustrated by the SEM image in Figure 3i,j (bottom). In the second example, the **TMal** photoresist was utilized to incorporate responsive features with spatial resolution into 3D materials (Figure 3k). Here, the **TMal** resist is combined with a classical resist to fabricate a 3D multi-material popsicle structure in a two-step writing process. Initially, a commercial acrylate-based resist (IP-S, Nanoscribe) was used to fabricate the base and popsicle-stick segments with a laser power and scan speed of 30 mW and 2000 µm s^{-1}, respectively. After washing away excess resist, the popsicle segment was printed from the **TMal** resist (laser power and scan speed of 20 mW and 1250 µm s^{-1}, respectively) and the final multi-material structure was evidenced by SEM imaging (Figure 3k, top). This example serves as a clear demonstration not only of **TMal** photoresist's compatibility with other resists but also of its ability to 3D print a new material around an existing 3D printed structure, thereby creating a hybrid 3D multi-material structure with responsive properties. After placing the popsicle in an oven at 150 °C for 24 h, SEM analysis was employed to confirm that only the popsicle segment undergoes de-cross-linking and "melts" thereby revealing the irreversibly printed "stick" (Figure 3k, bottom). Notably, the popsicle segment can be removed by immersing the final multi-material structure in DMSO for 24 h at 150 °C, highlighting the ability to completely remove the **TMal** resist in a single post-printing step if required (Figure S9, Supporting Information).

3. Conclusion

A new and initiator-free photoresist for DLW was introduced, simply comprising of a multifunctional compound and a solvent. The photoresist based on a photocycloaddition mechanism rather than conventional chain growth polymerization facilitated rapid fabrication of 3D microstructures above 1000 µm s^{-1} while maintaining printing quality, which can be degraded after printing with no necessity for additional (chemical) treatments except for exposure to elevated temperatures. Specifically, the mechanical properties of the printed structures were demonstrated to undergo significant changes when exposed to elevated temperatures, resulting from the de-cross-linking of the material. The structural change was further illustrated by fabricating thermally degradable 3D microstructures exclusively from the photoresist, as well as imparting bulk erasable features with spatial resolution into a 3D multi-material structure when combined with a commercially available photoresist. The thiomaleimide-based photoresist and its applicability to two-photon printing applications constitutes a critical advancement, particularly in terms of improved manufacturing speed, whereby 3D structures can be rapidly printed without relying on a photoinitiator, in combination with solvent-free post-printing de-cross-linking through simple exposure to elevated temperatures.

Supporting Information

Supporting Information is available from the Wiley Online Library or from the author.

Acknowledgements

C.B.-K. acknowledges the Australian Research Council (ARC) for a Laureate Fellowship enabling his photochemical research program. C.B.-K. and M.W. acknowledge funding from the Deutsche Forschungsgemeinschaft (DFG, German Research Foundation) under Germany's Excellence Strategy for the Excellence Cluster "3D Matter Made to Order" (EXC–2082/1 – 390761711). H.A.H. acknowledges funding from the European Union's Horizon 2020 research and innovation program under the EUTOPIA-SIF Marie Skłodowska-Curie grant agreement No. 945380, and the Royal Society for his University Research Fellowship (URF\R1\231098). The authors are grateful to Philip Scott (APA, KIT) for his assistance with FTIR Spectroscopy during the revision stage.

Conflict of Interest

The authors declare no conflict of interest.

Data Availability Statement

The data that support the findings of this study are available in the supplementary material of this article.

Keywords

3D laser printing, erasable structures, microstructures, photocycloaddition, photoinitiator-free, photoresists

Received: August 12, 2024
Revised: October 29, 2024
Published online:

[1] M. Carlotti, O. Tricinci, V. Mattoli, *Adv. Mater. Technol.* **2022**, *7*, 2101590.
[2] Z. Faraji Rad, P. D. Prewett, G. J. Davies, *Microsyst. Nanoeng.* **2021**, *7*, 71.
[3] L.-Y. Hsu, P. Mainik, A. Münchinger, S. Lindenthal, T. Spratte, A. Welle, J. Zaumseil, C. Selhuber-Unkel, M. Wegener, E. Blasco, *Adv. Mater. Technol.* **2023**, *8*, 2200801.
[4] S. Maruo, O. Nakamura, S. Kawata, *Opt. Lett.* **1997**, *22*, 132.
[5] J. Fischer, M. Wegener, *Laser Photonics Rev.* **2013**, *7*, 22.
[6] B.-B. Xu, Y.-L. Zhang, H. Xia, W.-F. Dong, H. Ding, H.-B. Sun, *Lab Chip.* **2013**, *13*, 1677.
[7] C. Delaney, J. Qian, X. Zhang, R. Potyrailo, A. L. Bradley, L. Florea, *J. Mater. Chem. C.* **2021**, *9*, 11674.
[8] B. Richter, V. Hahn, S. Bertels, T. K. Claus, M. Wegener, G. Delaittre, C. Barner-Kowollik, M. Bastmeyer, *Adv. Mater.* **2017**, *29*, 1604342.
[9] A. Koroleva, A. Deiwick, A. Nguyen, S. Schlie-Wolter, R. Narayan, P. Timashev, V. Popov, V. Bagratashvili, B. Chichkov, *PLoS One.* **2015**, *10*, e0118164.
[10] C. A. Spiegel, M. Hippler, A. Münchinger, M. Bastmeyer, C. Barner-Kowollik, M. Wegener, E. Blasco, *Adv. Funct. Mater.* **2020**, *30*, 1907615.
[11] D. Gräfe, A. Wickberg, M. M. Zieger, M. Wegener, E. Blasco, C. Barner-Kowollik, *Nat. Commun.* **2018**, *9*, 2788.
[12] M. M. Zieger, P. Müller, E. Blasco, C. Petit, V. Hahn, L. Michalek, H. Mutlu, M. Wegener, C. Barner-Kowollik, *Adv. Funct. Mater.* **2018**, *28*, 1801405.
[13] D. Gräfe, S. L. Walden, J. Blinco, M. Wegener, E. Blasco, C. Barner-Kowollik, *Angew. Chem.* **2020**, *59*, 6330.
[14] J. Houghtaling, T. Liang, G. Thiessen, E. Fu, *Anal. Chem.* **2013**, *85*, 11201.
[15] Y. Jia, C. A. Spiegel, A. Welle, S. Heißler, E. Sedghamiz, M. Liu, W. Wenzel, M. Hackner, J. P. Spatz, M. Tsotsalas, E. Blasco, *Adv. Funct. Mater.* **2023**, *33*, 2207826.
[16] F. Mayer, D. Ryklin, I. Wacker, R. Curticean, M. Čalkovský, A. Niemeyer, Z. Dong, P. A. Levkin, D. Gerthsen, R. R. Schröder, M. Wegener, *Adv. Mater.* **2020**, *32*, 2002044.
[17] J. Zhou, X. Allonas, A. Ibrahim, X. Liu, *Prog. Polym. Sci.* **2019**, *99*, 101165.
[18] A. Bagheri, J. Jin, *ACS Appl. Polym. Mater.* **2019**, *1*, 593.
[19] M. Rothammer, D. T. Meiers, M. Maier, G. von Freymann, C. Zollfrank, *J. Opt. Soc. Am. B.* **2023**, *40*, 849.
[20] B. T. Benkhaled, K. Belkhir, T. Brossier, C. Chatard, A. Graillot, B. Lonetti, A.-F. Mingotaud, S. Catrouillet, S. Blanquer, V. Lapinte, *Eur. Polym. J.* **2022**, *179*, 111570.
[21] H. A. Houck, P. Müller, M. Wegener, C. Barner-Kowollik, F. E. Du Prez, E. Blasco, *Adv. Mater.* **2020**, *32*, 2003060.
[22] D. Song, A. Husari, F. Kotz-Helmer, P. Tomakidi, B. E. Rapp, J. Rühe, *Small.* **2024**, *20*, 2306682.
[23] M. V. Tsurkan, C. Jungnickel, M. Schlierf, C. Werner, *J. Am. Chem. Soc.* **2017**, *139*, 10184.
[24] S. C. Gauci, M. Gernhardt, H. Frisch, H. A. Houck, J. P. Blinco, E. Blasco, B. T. Tuten, C. Barner-Kowollik, *Adv. Funct. Mater.* **2022**, *33*, 2206303.
[25] S. C. Gauci, K. Ehrmann, M. Gernhardt, B. Tuten, E. Blasco, H. Frisch, V. Jayalatharachchi, J. P. Blinco, H. A. Houck, C. Barner-Kowollik, *Adv. Mater.* **2023**, *35*, 2300151.
[26] F. Pashley-Johnson, R. Munaweera, S. I. Hossain, S. C. Gauci, L. Delafresnaye, H. Frisch, M. L. O'Mara, F. E. D. Prez, C. Barner-Kowollik, *Nat. Commun.* **2024**, *15*, 6033.
[27] S. C. Gauci, A. Vranic, E. Blasco, S. Bräse, M. Wegener, C. Barner-Kowollik, *Adv. Mater.* **2024**, *36*, 2306468.
[28] P. Froimowicz, H. Frey, K. Landfester, *Macromol. Rapid Commun.* **2011**, *32*, 468.
[29] S. R. Trenor, T. E. Long, B. J. Love, *Macromol. Chem. Phys.* **2004**, *205*, 715.
[30] Y. Inaki, H. Hiratsuka, *JPST.* **2000**, *13*, 739.
[31] G. Kaur, P. Johnston, K. Saito, *Polym. Chem.* **2014**, *5*, 2171.
[32] L. M. Tedaldi, A. E. Aliev, J. R. Baker, *Chem. Commun.* **2012**, *48*, 4725.
[33] R. Malde, M. A. Parkes, M. Staniforth, J. M. Woolley, V. G. Stavros, V. Chudasama, H. H. Fielding, J. R. Baker, *Chem. Sci.* **2022**, *13*, 2909.
[34] M. Aljuaid, Y. Chang, D. M. Haddleton, P. Wilson, H. A. Houck, *J. Am. Chem. Soc.* **2024**, *146*, 19177.
[35] M. Aljuaid, H. A. Houck, S. Efstathiou, D. M. Haddleton, P. Wilson, *Macromol.* **2022**, *55*, 8495.
[36] L. Yang, A. Münchinger, M. Kadic, V. Hahn, F. Mayer, E. Blasco, C. Barner-Kowollik, M. Wegener, *Adv. Optical Mater.* **2019**, *7*, 1901040.